ACCOUNTS
of chemical research

Organic Semiconductors Based on [1]Benzothieno[3,2-*b*][1]benzothiophene Substructure

Kazuo Takimiya,*,[†,‡] Itaru Osaka,[†] Takamichi Mori,[†,‡] and Masahiro Nakano[†]

[†]Emergent Molecular Function Research Group, RIKEN Center for Emergent Matter Science (CEMS), Wako, Saitama 351-0198, Japan

[‡]Department of Applied Chemistry, Graduate School of Engineering, Hiroshima University, Higashi-Hiroshima 739-8527, Japan

Supporting Information

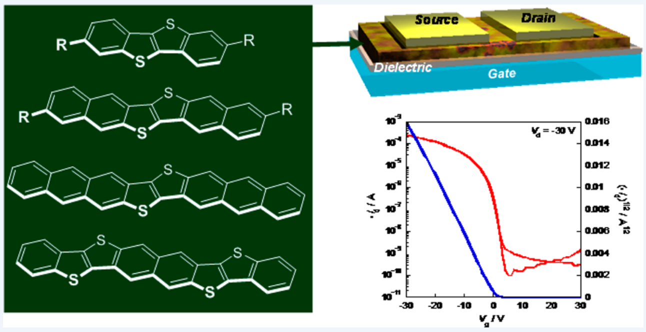

CONSPECTUS: The design, synthesis, and characterization of organic semiconductors applicable to organic electronic devices, such as organic field-effect transistors (OFETs) and organic photovoltaics (OPVs), had been one of the most important topics in materials chemistry in the past decade. Among the vast number of materials developed, much expectation had been placed on thienoacenes, which are rigid and planar structures formed by fusing thiophenes and other aromatic rings, as a promising candidate for organic semiconductors for high-performance OFETs. However, the thienoacenes examined as an active material in OFETs in the 1990s afforded OFETs with only moderate hole mobilities (approximately 0.1 $cm^2\ V^{-1}\ s^{-1}$). We speculated that this was due to the sulfur atoms in the thienoacenes, which hardly contributed to the intermolecular orbital overlap in the solid state. On the other hand, we have focused on other types of thienoacenes, such as [1]benzothieno[3,2-*b*][1]benzothiophene (BTBT), which seem to have appropriate HOMO spatial distribution for effective intermolecular orbital overlap. In fact, BTBT derivatives and their related materials, including dinaphtho[2,3-*b*:2′,3′-*f*]thieno[3,2-*b*]thiophene (DNTT), have turned out to be superior organic semiconductors, affording OFETs with very high mobilities. To illustrate some examples, we have developed 2,7-diphenyl BTBT (DPh-BTBT) that yields vapor-deposited OFETs having mobilities of up to 2.0 $cm^2\ V^{-1}\ s^{-1}$ under ambient conditions, highly soluble dialkyl-BTBTs (C_n-BTBTs) that afford solution-processed OFETs with mobilities higher than 1.0 $cm^2\ V^{-1}\ s^{-1}$, and DNTT and its derivatives that yield OFETs with even higher mobilities (>3.0 $cm^2\ V^{-1}\ s^{-1}$) and stability under ambient conditions. Such high performances are rationalized by their solid-state electronic structures that are calculated based on their packing structures: the large intermolecular orbital overlap and the isotropic two-dimensional electronic structure are the key regardless of the molecular size and substituents on the BTBT and its related thienoacene cores. Along with the discovery of such attracting performances, versatile and practical methods for the synthesis of BTBT and its derivatives, and the π-extended derivatives including DNTT, dianthra[2,3-*b*:2′,3′-*f*]thieno[3,2-*b*]thiophene (DATT), and the thienoacenes with two thieno[3,2-*b*]thiophene moieties, have been developed. In addition, the materials have been recently utilized in sophisticated devices and circuits, including all-printed transistor arrays, flexible circuits on ultrathin plastic substrates, and biomedical applications, underscoring their promise as practical semiconductors for electronic device applications. These exciting results of the present BTBT-based materials are expected to open doors to new horizons of organic semiconductors in terms of practical application and the design and synthesis of far more superior materials.

1. INTRODUCTION

The synthesis and characterization of organic semiconductors have been a focal research field in the last two decades. Their potential application to large-area and flexible electronic devices, such as organic field-effect transistors (OFETs), organic light-emitting diodes (OLEDs), and organic photovoltaics (OPVs), has sparked intensive research in this field.[1] OFETs are a fundamental device that is used as the backplane of various displays, radio frequency ID tags, sensors, switches, and so forth.[2] Although the carrier mobilities, which are the most important figure of merit in field-effect transistors of any kind, were far lower in OFETs than in silicon-based transistors until the 1990s, continuous and intensive research geared toward both materials development and device optimization has led to significant improvements in OFET performance. For example, pentacene-based devices, which were reported in 1992 to have mobilities of approximately $2 \times 10^{-3}\ cm^2\ V^{-1}\ s^{-1}$,[3] have today achieved mobilities comparable to or exceeding those of amorphous-silicon-based FETs.[4] From the materials viewpoint, highly extended polyacenes, a representative example of which is pentacene,[4] are prototypical organic semiconductors that

Received: November 26, 2013
Published: May 1, 2014

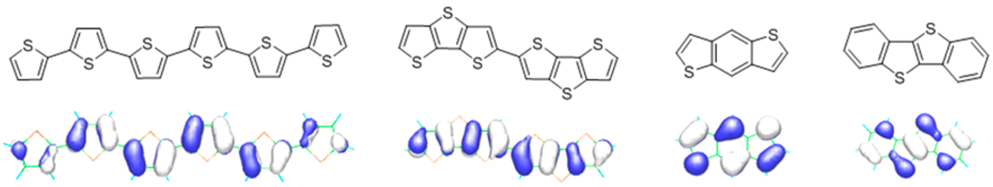

Figure 1. HOMOs of α-6T, BDTT, BDT, and BTBT (calculated with DFT B3LYP/6-31g(d)).

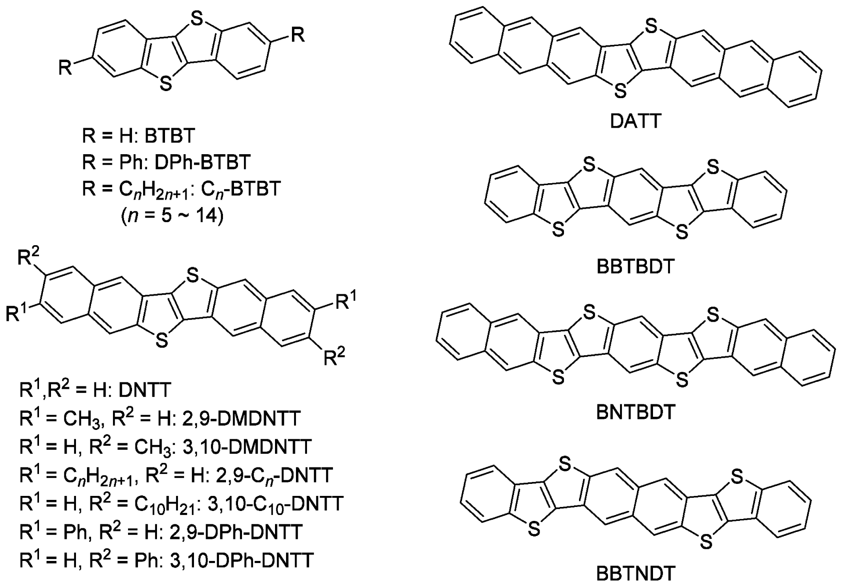

Figure 2. Molecular structures of BTBT and related organic semiconductors.

have driven the field of organic electronics in the past decade.[5] Unfortunately, however, although the carrier mobilities of such polyacene-based OFETs are generally high, their low chemical stability is a drawback. Thus, the stabilization of pentacene and related compounds by chemical modification is one of the promising approaches to developing superior organic semiconductors.[6] On the other hand, many different material classes with extended π-conjugation frameworks have also been examined as the active material in OFETs to achieve high mobility and stability.[7]

Mobility enhancement and environmental robustness to oxidation in ambient air are the two major requirements of organic semiconductors for OFETs. For the development of air-stable p-channel organic semiconductors, lowering the HOMO energy level (E_{HOMO}) while keeping it suitable to hole injection from an electrode is a feasible strategy.[8] On the other hand, mobility enhancement has not been an easy task. Among the many material classes examined, π-extended heteroaromatics seem to be promising because carrier transport in the molecular solid is governed by intermolecular orbital overlap[9] and heteroatoms, such as sulfur that has a larger atomic radius than carbon, are expected to facilitate intermolecular nonbonded interaction and therefore orbital overlaps. In fact, many thiophene-based organic semiconductors, including π-extended oligothiophenes and fused-thiophene compounds (thienoacenes), for example, α-sexithiophene (α-6T),[10] α,α'-bis(dithieno[3,2-*b*:2′,3′-*d*]thiophene) (BDTT),[11a] and α,α'-bis(benzo[1,2-*b*:4,5-*b*′]dithiophene) (BBDT),[11b] have been developed and examined as the active material for OFETs since the late 1990s. However, few thiophene-based organic semiconductors afforded OFETs with mobilities higher than or comparable to those of pentacene-based ones.

Although the performances of thiophene-based organic semiconductors reported before 2000 were unremarkable, we were interested in those materials, particularly their electronic structures. To gain an insight into those compounds, molecular orbital (MO) calculations of several thiophene-based materials, such as α-6T, BDTT, benzo[1,2-*b*:4,5-*b*′]dithiophene (BDT), and [1]benzothieno[3,2-*b*][1]benzothiophene (BTBT), were carried out. The spatial distributions of their HOMOs (Figure 1) show that there is virtually no contribution of sulfur atoms to the HOMOs of α-6T and BDTT. In other words, nodal planes exist on the sulfur atoms, implying negligible contribution of the sulfur atoms to the intermolecular HOMO overlap. In contrast, the sulfur atoms make a large contribution to the HOMO of BTBT, suggesting effective contribution of the sulfur atoms to the intermolecular HOMO overlap for carrier transport. Although this could be a rather simple hypothesis, we thought it would be interesting to examine such thienoacenes as BTBT as organic semiconductors for OFETs.

The molecular structure of BTBT was elucidated as early as in 1949, when Horton discussed the possible products in the thermal reaction of toluene and elemental sulfur.[12] Thereafter, several BTBT derivatives, including the parent BTBT, were synthesized in the 1980s.[13−18] Those early works on the BTBT derivatives were mainly motivated by their potential use as liquid crystalline materials.[15] In 2004, we made the first attempt to fabricate parent-BTBT-based OFETs by vapor deposition, but the attempt met with failure owing to the poor film-forming property of the parent BTBT. The first material to successfully afford working OFETs was 2,7-diphenyl-BTBT (DPh-BTBT); its vapor-processed OFETs showed mobilities of up to 2.0 cm^2

Scheme 1. Representative Synthetic Routes to BTBT and Its Derivatives

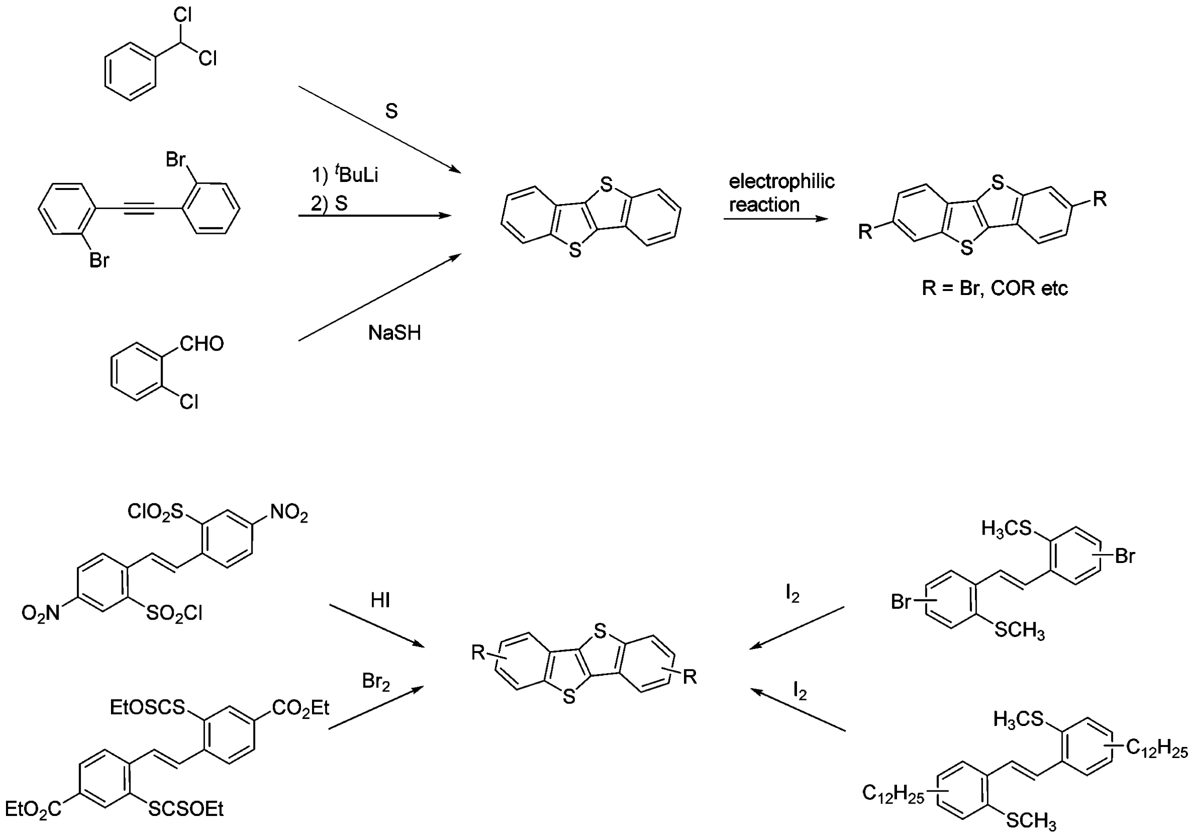

Scheme 2. Synthesis of DNTT and Its Derivatives

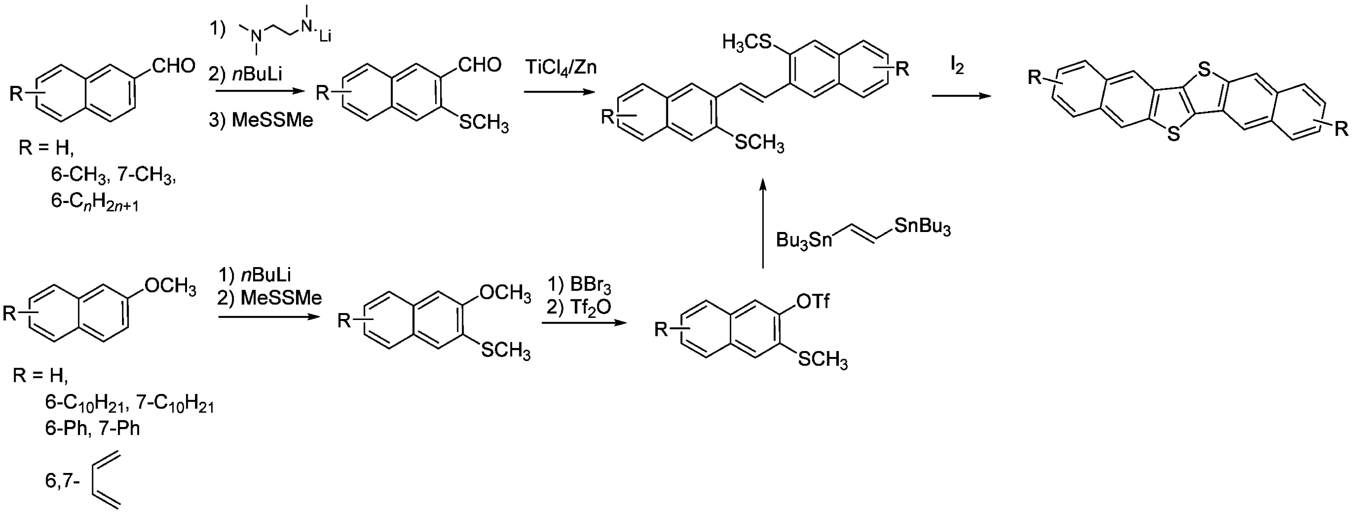

V^{-1} s^{-1} under ambient conditions.[19] Since then, various BTBT derivatives[20,21] and π-extended BTBT analogues, such as dinaphtho[2,3-*b*:2′,3′-*f*]thieno[3,2-*b*]thiophene (DNTT),[22] have been synthesized and evaluated as organic semiconductors for OFET devices (Figure 2), and most of them have turned out to be superior organic semiconductors, affording OFETs with high mobilities. Furthermore, several materials in this class have found use in sophisticated device applications.[23] The importance of this class of organic semiconductors has prompted us to review the synthesis and materials variation, device characteristics, crystal structures, and electronic structures of BTBT and related organic semiconductors.

2. SYNTHESIS AND MATERIALS VARIATION

Various methods for the synthesis of BTBT derivatives from different starting compounds have been reported (Scheme 1).[13−18] Parent BTBT, which can be conveniently synthesized in a single step from commercial starting materials in a large quantity (>30 g),[13,14] can also be selectively functionalized at the 2,7-positions via an electrophilic substitution reaction to provide a range of derivatives. Of particular importance are diacyl BTBTs, which can be converted into the corresponding dialkyl-BTBTs (C_n-BTBTs) to afford solution-processed OFETs with high mobilities (vide infra).[20] Stilbenes with *o*-sulfur functional groups can also be converted into correspond-

Scheme 3. Two Synthetic Approaches to Largely π-Extended Compounds with Two Thieno[3,2-*b*]thiophene Moieties

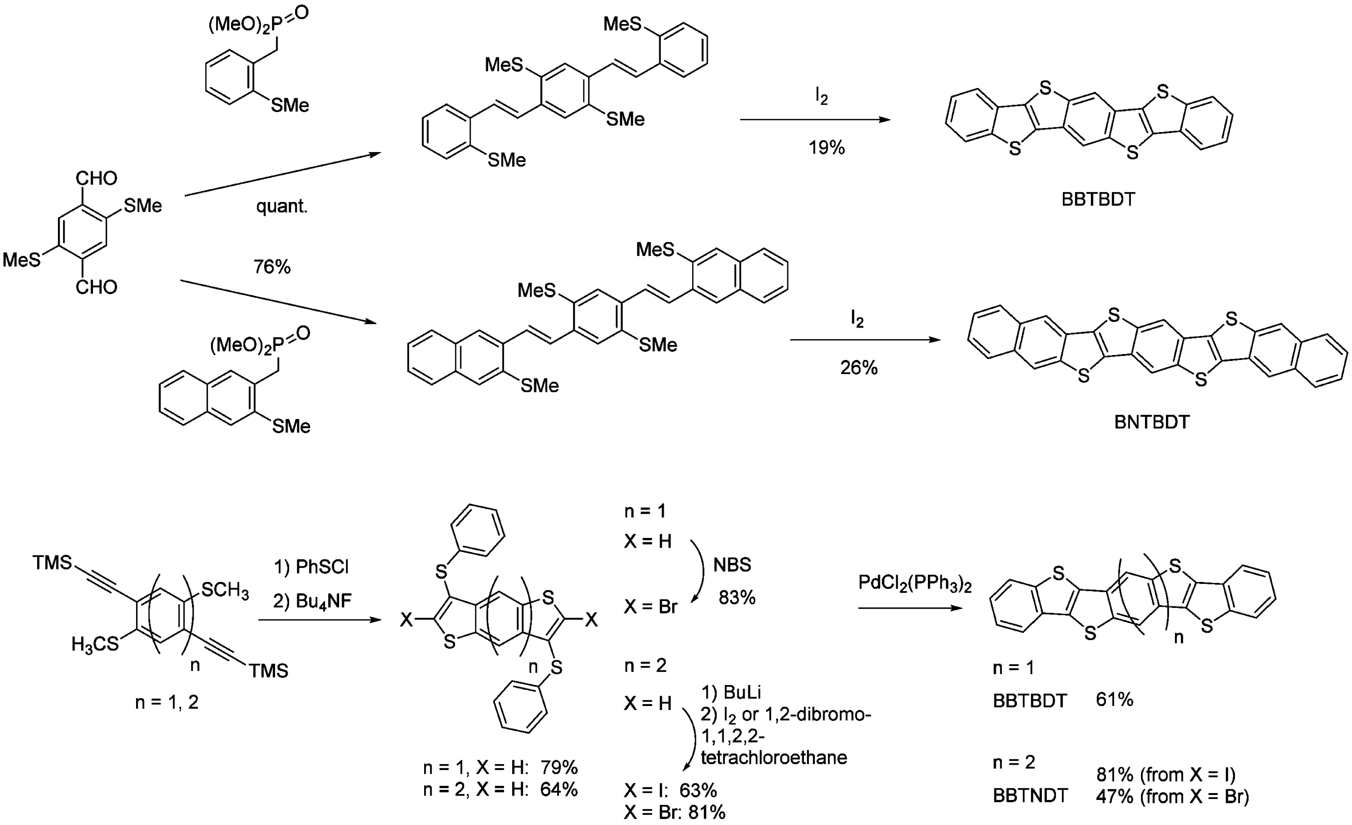

ing BTBT derivatives with a range of substituents, such as nitro,[16] ester,[17] bromo,[18] and alkyl groups.[18] Of them, 2,7-dinitro-BTBT can be reduced into the corresponding diamino-BTBT, which, via the diazotization reaction, is converted into the diiodo-BTBT, a versatile intermediate for the synthesis of DPh-BTBT[19] and C$_n$-BTBTs.[20]

For the synthesis of DNTT derivatives, the iodine-promoted thienothiophene formation from *trans*-1,2-bis(3-methylthio-naphthalen-2-yl)ethene intermediates is a workhorse reaction (Scheme 2).[22] The precursors of DNTT and its derivatives can be conveniently synthesized from the corresponding 3-methylthio-2-naphthaldehydes via a low-valence titanium-mediated coupling reaction.[24] Although the introduction of the 3-methylthio substituent on 2-naphthaldehyde can be easily done, a concomitant 1-methylthiolated isomer should be removed from the reaction mixture by column chromatography, which hinders its application to scalable synthesis. Alternatively, 2-methoxynaphthalenes are versatile starting materials in the synthesis of DNTT derivatives.[25] After selective introduction of the methylthio moiety at the 3-position of 2-methoxynaphthalenes, conversion of the 2-methoxy into the trifluoromethanesulfonate functionality followed by the Stille-cross coupling reaction with *trans*-1,2-bis(tributylstannyl)-ethene gives the corresponding bis(3-methylthionaphthalen-2-yl)ethenes. The latter synthetic route to the precursors of DNTTs is superior to the former one in terms of easy experimental operation (no chromatographic separation of the isomer is necessary), cost of starting materials, scalability, and total yield (79% for the latter vs 39% total yield for the former in the synthesis of parent DNTT). Taking advantage of those merits, the use of various 2-methoxynaphthalenes with a substituent at the 6- and/or 7-postion has allowed us to synthesize new DNTT derivatives, including 2,9- and 3,10-diphenyl- and 3,10-didecyl-DNTT,[25] and π-extended dianthra-[2,3-*b*:2′,3′-*f*]thieno[3,2-*b*]thiophene (DATT).[26]

Further π-extended materials with two thieno[3,2-*b*]-thiophene moieties were also synthesized via the double iodine-promoted thienothiophene formation or via a consecutive thiophene annulation approach (Scheme 3).[27] Poor access to the precursors having two *o*-bis(methylthio)stilbene moieties and low synthetic yields at the final step are the two major drawbacks of the former method. In contrast, the latter method affords straightforward access to BBTBDT and BBTNDT from readily available starting materials and reagents.[27b]

3. MOLECULAR PROPERTIES AND FET PERFORMANCES

HOMO Energy Levels

As the E_{HOMO} is one of the most important molecular properties of p-channel organic semiconductors, E_{HOMO}'s of all the BTBT-based compounds were evaluated by cyclic voltammetry (CV) in solution and/or by photoelectron spectroscopy in air (PESA) in the thin film state (Table 1). In general, the E_{HOMO}'s evaluated by CV and PESA are in good agreement for many material classes, including acenes and thienoacenes. This is also the case for the present materials, for example, BTBT, DPh-BTBT, and DNTT. However, it is interesting to note that the compounds with long alkyl groups, C$_n$-BTBTs and C$_n$-DNTTs, tend to give markedly high-lying E_{HOMO}'s in the PESA evaluations. Although such large differences in the experimental E_{HOMO}'s, depending on the evaluation method, cannot be clearly explained, it is speculated that the strong intermolecular electronic interaction between

Table 1. E_{HOMO}'s and E_g's of Representative BTBT-Based Organic Semiconductors

	E_{HOMO}/eV		E_g/eV[c]	
compd	CV[a]	PESA[b]	solution	thin film
BTBT	−5.8	−5.8	3.6	
C_n-BTBT (n = 5−14)	−5.7	−5.3	3.5	3.3
DPh-BTBT	−5.6	−5.6	3.3	3.0
DNTT	−5.4	−5.4	2.9	2.6
2,9-C_{10}-DNTT	−5.4	−4.9	2.9	2.6
2,9-DPh-DNTT		−5.3	2.7	2.4
DATT		−5.1	2.4	2.1
BBTBDT		−5.2	3.1	2.8
BNTBDT		−5.2	2.7	2.4
BBTNDT		−5.1[d]	2.7	2.4

[a] Determined from the onset potential in CVs measured in the solution. [b] Determined by photoemission yield spectroscopy in air (PESA) with a RIKEN KEIKI AC-2 surface analyzer. [c] Calculated from λ_{edge} of absorption spectra.

the adjacent molecules in the well-ordered thin film state assisted by the long alkyl groups lowers the effective E_{HOMO}'s in the thin film state.[28a]

The E_{HOMO}'s of the present compounds are low compared with the E_{HOMO}'s of the corresponding linear acenes having the same number of aromatic rings. As an example, E_{HOMO} of tetracene is 5.2 eV below the vacuum level, whereas E_{HOMO} of parent BTBT is 5.8 eV. This marked difference is ascribed to the electronic structures of the two compounds. Despite the fact that the molecular structure of BTBT, which consists of four aromatic rings fused in a linear manner, is, at first glance, quite similar to that of tetracene, the thiophene rings incorporated in the middle of the fused-ring system correspond to the phene-like electronic structure, resulting in the effective stabilization of E_{HOMO}.[29] The difference in the HOMO−LUMO energy gaps (E_g's in Table 1) between BTBT and tetracene (3.6 and 2.5 eV, respectively, as estimated from the absorption onset in the solution spectra) can also be ascribed to the difference in the electronic structures. Similarly, E_{HOMO}'s of compounds with an even larger number of fused aromatic rings are kept relatively low, that is, as low as −4.9 eV, which is beneficial for realizing stable OFETs operable under ambient conditions.

FET Characteristics: Mobility

The most important feature of the present materials is that they generally yield transistors with excellent mobilities regardless of the molecular size or the substituent (Table 2). Even the smallest molecular class, the BTBT derivatives, can afford OFETs with mobilities higher than 1.0 $cm^2 V^{-1} s^{-1}$.[19−21] It is also worth mentioning that C_n-BTBTs, which are highly soluble in common organic solvents (~90 g L^{-1} in chloroform at room temperature), can afford solution-processed OFETs showing excellent device performance with mobilities higher than 1.0 $cm^2 V^{-1} s^{-1}$ in various device configurations fabricated by different deposition processes.[20,30] The most prominent result reported recently is the fabrication of C_8-BTBT-based devices by a double-shot inkjet technique, thereby allowing the formation of high-quality single-crystal-like thin films. The crystalline films can act as a superior semiconductor channel to produce OFETs with mobility of 16 $cm^2 V^{-1} s^{-1}$ on average.[30e]

Parent DNTT is also a promising organic semiconductor. It is used in the fabrication of high-performance OFETs with mobilities as high as 3 $cm^2 V^{-1} s^{-1}$ by vapor processes, and can afford semiconducting channels regardless of the substrate or the device configuration. Some examples are single-crystal transistors,[31] OFETs with a vertical three-dimensional (3D) channel structure,[32a] carbon nanotube enabled vertical OFETs,[32b] and devices and circuits fabricated on alkylphosphate-SAM on flexible plastic substrates.[32c] Slightly higher mobilities (~3.5 $cm^2 V^{-1} s^{-1}$) than those of the parent-DNTT-based devices were recorded by DPh-DNTT-based OFETs.[25] On the other hand, field-effect mobility was further enhanced by the alkylation of DNTT; 2,9-C_{10}-DNTT-based OFETs fabricated by vapor deposition showed impressively high mobilities of up to 8 $cm^2 V^{-1} s^{-1}$,[24] which are among the highest for OFETs that are based on a polycrystalline thin film. Further π-extended analogues having more than six aromatic ring systems also afforded similar device characteristics, for

Table 2. OFET Characteristics of Representative BTBT-Based Materials

compd	T_{sub}/°C[a]	μ/$cm^2 V^{-1} s^{-1}$[b]	I_{on}/I_{off}	note[c]	ref
DPh-BTBT	100	2.0	10^7	TC, OTS-SAM	19
C_n-BTBT (n = 5−14)		2.8	10^7	TC, spin coating, annealed at 80 °C	20a
C_{12}-BTBT	rt	3.9	10^6−10^8	TC, ODTS-SAM	20b
C_8-BTBT		5	10^6	TC, DTS-SAM, directing crystallization	30d
C_8-BTBT		31	10^5−10^7	TG, CYTOP dielectric, double-shot ink jet	30e
DNTT	60	2.9	10^7	TC, OTS-SAM	22
DNTT		8.3	10^8	SC, TC, CYTOP dielectric	31
DNTT	60	0.6	10^6	TC, AlO_x dielectric, n-tetradecylphosphonic acid-SAM, V_d = −1.5 V, V_g = 0 ~ −3 V	32c
2,9-C_n-DNTT (n = 6, 8, 10, 12)	60	0.7−3.7	10^7−10^9	TC without SAM	24
2,9-C_{10}-DNTT	60	7.9	10^8	TC, ODTS-SAM	24
2,9-DPh-DNTT	100	3.4	10^8	TC, OTS-SAM	34
3,10-DPh-DNTT	100	3.6	10^8	TC, ODTS-SAM	34
DATT	100	3.0	10^6	TC, ODTS-SAM	26
BBTBDT	100	5.6	10^7	TC, ODTS-SAM	27b

[a] Substrate temperature during deposition. [b] Extracted from the saturation regime using vapor-deposited thin-film OFETs fabricated on Si/SiO_2 substrates unless otherwise stated. [c] TC: top-contact device, TG: top-gate device, SC: single-crystal transistor, OTS: octyltrichlorosilane, ODTS: octadecyltrichlorosilane, DTS: decyltriethoxysilane, SAM: self-assembled monolayer.

example, 3.0 cm^2 V^{-1} s^{-1} for DATT[26] and 5.6 cm^2 V^{-1} s^{-1} for BBTNDT.[27b]

FET characteristics: Operation under Ambient Conditions

As expected from the relatively low-lying E_{HOMO}'s (4.9−5.7 eV below the vacuum level, see Table 1), one of the notable features of the present OFETs is their ability to operate in ambient air, which is a merit for practical use compared with the pentacene-based devices. On the other hand, the devices made with the present materials have often suffered from large contact resistance between the source electrode and the semiconducting layer, particularly the devices with very short channel length (L, less than 10 μm). Thus, contact doping techniques were examined to compensate the large injection barrier and found to be very effective for the fabrication of devices with short L and their integrated circuits, enabling high-frequency operation.[33]

For practical application to integrated electronic devices, such as driving circuits for displays or biomedical sensors,[23] thermal stability at the device stage is another requirement of practical OFETs. In this context, BTBT and DNTT derivatives having long alkyl groups may not be promising owing to their thermal phase transition into the liquid crystalline phase at relatively low temperatures (∼120 °C). In fact, thermal treatment of the devices with C_n-BTBTs and C_n-DNTTs above the phase transition temperatures significantly degrades the device characteristics.[34] On the contrary, parent DNTT, which does not show any thermal phase transition up to 300 °C, was found to afford thermally stable OFETs on both Si/SiO$_2$ and flexible plastic substrates up to 160 °C, though significant degradation of the device characteristics were observed above 160 °C owing to thermally induced structural change in the crystal grains on the substrate.[23a,34] Further improved thermal stability up to the temperature of 250 °C was recently found in DPh-DNTT-based OFETs,[34,35] particularly 2,9-DPh-DNTT, which, in combination with the high mobility (∼3.5 cm^2 V^{-1} s^{-1}), makes the material a useful organic semiconductor for many practical applications in the future. In addition to those large molecules, the unsymmetrical substitution on the small BTBT core was also proven to improve thermal stability; 2-(octylthiophen-2-yl)-substituted BTBT having a highly ordered liquid crystalline phase afforded solution-processed OFETs with mobilities higher than 1 cm^2 V^{-1} s^{-1}, which were stable up to 150 °C.[21a]

4. CRYSTAL STRUCTURES AND ELECTRONIC STRUCTURES IN THE SOLID STATE

Packing Structure in the Solid State

The mobilities of OFET devices are not only a molecular property but also a device characteristic that is affected by several factors, including crystallinity, molecular orientation, film uniformity, and connectivity between crystalline grains. In general, the materials discussed here afford uniform, polycrystalline thin films by vapor deposition or spin coating from solution on the substrates (Figure 3).

In the thin films deposited on the substrates, the BTBT-based materials tend to have edge-on, lamella-like packing structures that are easily detected by out-of-plane XRD measurements with conventional laboratory equipment. Furthermore, in-plane XRD often affords useful information on the packing structure in each lamellar layer and that information corroborates the structural information from single-crystal XRD. A typical example is shown in Figure 4 for C$_{10}$-DNTT.

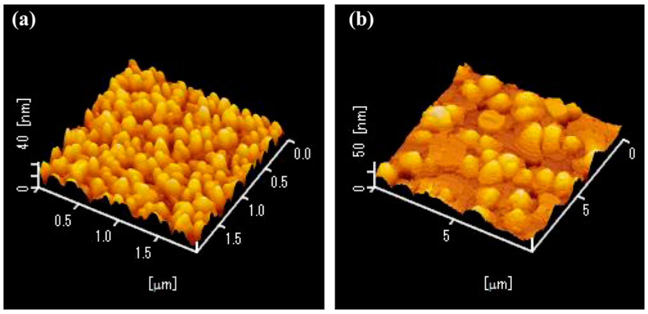

Figure 3. AFM images of evaporated thin film of DNTT (a) and spin-coated thin film of C$_8$-BTBT (b).

In the out-of-plane XRD, a series of peaks assignable to 00*l* diffractions are observed (Figure 4a). The extracted *d*-spacing is ca. 38 Å, which corresponds to the length of the crystallographic *c*-axis in the single-crystal cell (Figure 4c). On the other hand, in the in-plane XRD, three characteristic peaks are detected, which can be indexed as 110, 020, and 120 reflections by the single-crystal cell, indicating that the packing structure in the thin film state is basically the same as that in the single-crystal structure (Figure 4b).

As demonstrated in Figure 4d, the molecular arrangement in each layer is classified as the herringbone structure, which consists of two types of bimolecular pairs: edge-to-edge pairs (stacking pair) in the crystallographic *a*-axis direction and edge-to-face pairs in the crystallographic 110 and −110 directions. In general, compared with the edge-to-face pairs, intermolecular orbital coupling in the edge-to-edge pairs is smaller in other material classes, including acenes[36] and acenedithiophenes, because of the less effective intermolecular contacts through the molecular edges. In the case of the present herringbone structure, on the contrary, sulfur atoms at the thienothiophene moiety in the ladder-shaped molecules can effectively interact intermolecularly. Furthermore, the large contribution of the sulfur atoms to the HOMO can lead to effective intermolecular HOMO overlap, resulting in large intermolecular transfer integrals (t_{stacking}, Figure 4d). As a result, in combination with similarly effective HOMO overlap in the edge-to-face molecular pairs ($t_{\mathrm{transverse}}$), a two-dimensional (2D) electronic structure is realized in the semiconducting channel.

Inspection of Packing Structures

As most of the BTBT-based materials have similar herringbone structures to 2,9-C$_{10}$-DNTT, the effective HOMO overlap and the 2D electronic structure is expected to be the general features. However, detailed comparison of a range of compounds reveals several variations in the packing structures and hence the electronic structures depending on the molecule. To elucidate the relationship between the molecular factors, such as the size and substituent of molecules, and the orbital overlap of HOMOs (t's), we extracted the intermolecular distance between the molecular centroids (d_{stacking} and $d_{\mathrm{transverse}}$) in both edge-to-edge and edge-to-face pairs, respectively, and herringbone angle (dihedral angels between the molecular planes in edge-to-face pair) (Figure 5 and Table 3).

It is interesting to note that d_{stacking}'s of parent BTBT, DNTT, and DATT in the edge-to-edge pair increase with the size of molecule, whereas $d_{\mathrm{transverse}}$'s in the edge-to-face pairs are almost constant. This anisotropic change can qualitatively be understood by considering the fact that molecular width, the actual spread in the molecular short-axis direction, also

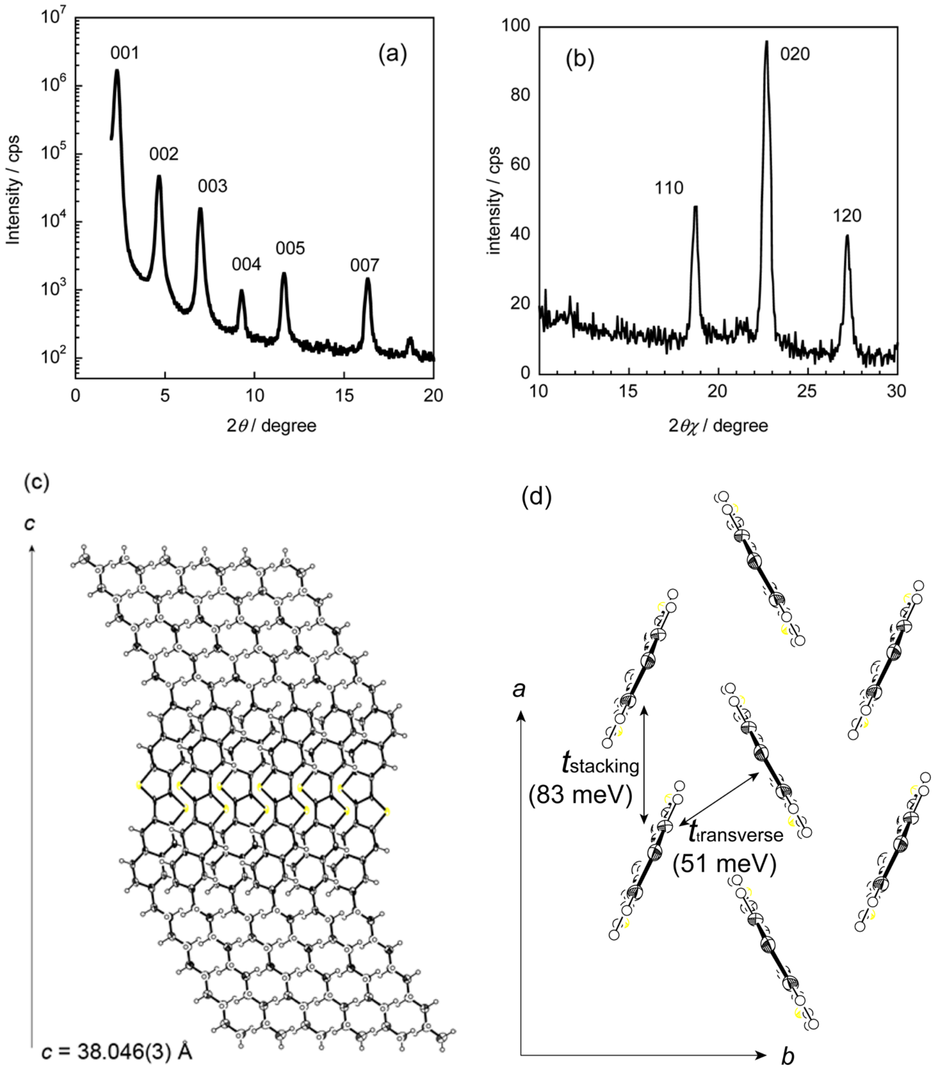

Figure 4. Characterization of solid-state structure of 2,9-C_{10}-DNTT by XRD measurements. Out-of-plane (a) and in-plane (b) XRDs of thin film, and packing structure elucidated by single-crystal XRD (c and d).

increases with the extension owing to the kinked molecular structures, which makes the molecular centroids apart in the edge-to-edge pair. Despite the increase of d_{stacking}'s, the calculated $t_{stacking}$'s are larger for DNTT and DATT than for BTBT, indicating that the extension of the conjugated system is generally beneficial to enhance the intermolecular orbital overlap. This is also the case in the edge-to-face pair; comparing $t_{\text{transverse}}$ of BTBT and the averaged $t_{\text{transverse}}$'s for DNTT and DATT, we find that the latter two are apparently larger. Another noticeable feature in the parent system is that $t_{\text{transverse}}$'s for DNTT and DATT are significantly influenced by $d_{\text{transverse}}$'s. Owing to the low symmetry of the unit cells (space group: $P2_1$ for both), there exist two different edge-to-face pairs with different $d_{\text{transverse}}$'s. As expected, the bimolecular pairs with shorter $d_{\text{transverse}}$ afford larger $t_{\text{transverse}}$'s in both DNTT and DATT. Although the herringbone angle is often referred to characterize the herringbone structure, no clear relationship between the angles and $t_{\text{transverse}}$'s are observed in the parent system as well as the derivatives.

The introduction of long alkyl groups generally reduce one or both of d_{stacking} and $d_{\text{transverse}}$, resulting in large t's compared with the parent system.[28b] This can be explained by the intermolecular van der Waals interaction of the long alkyl groups, called the "zipper effect,"[28] which brings about tight packing in the solid state. This in fact leads to a higher mobility for the 2,9-C_{10}-DNTT-based devices than for the parent-DNTT-based devices. In contrast, the introduction of phenyl groups leads to relatively loose packing; in DPh-BTBT, d_{stacking} is 6.33 Å, which is longer than that in the parent BTBT, resulting in smaller t_{stacking} (34 meV), although the close mutual position and the large $t_{\text{transverse}}$ are preserved in the edge-to-face pairs. The much longer d_{stacking} (6.99 Å) observed for 3,10-DPh-DNTT well corresponds to the smallest t_{stacking} (22 meV) among the present compounds, resulting in a rather anisotropic electronic structure. The increase in d_{stacking} by the introduction of phenyl groups is attributed to the increase in width of the molecules caused by the introduction of the phenyl groups and the relatively large dihedral angles between the central BTBT or the DNTT core and the phenyl groups (26.1° for DPh-BTBT and 29.3° for 3,10-DPh-DNTT, respectively). On the contrary, such structural perturbation by the phenyl groups is somehow relaxed in 2,9-DPh-DNTT, which contains two phenyl groups almost on the molecular long axis, and has smaller dihedral angles between the core and the phenyl substituents (25.2°). These structural factors could be the reason for the well-balanced 2D electronic structure in 2,9-DPh-DNTT.

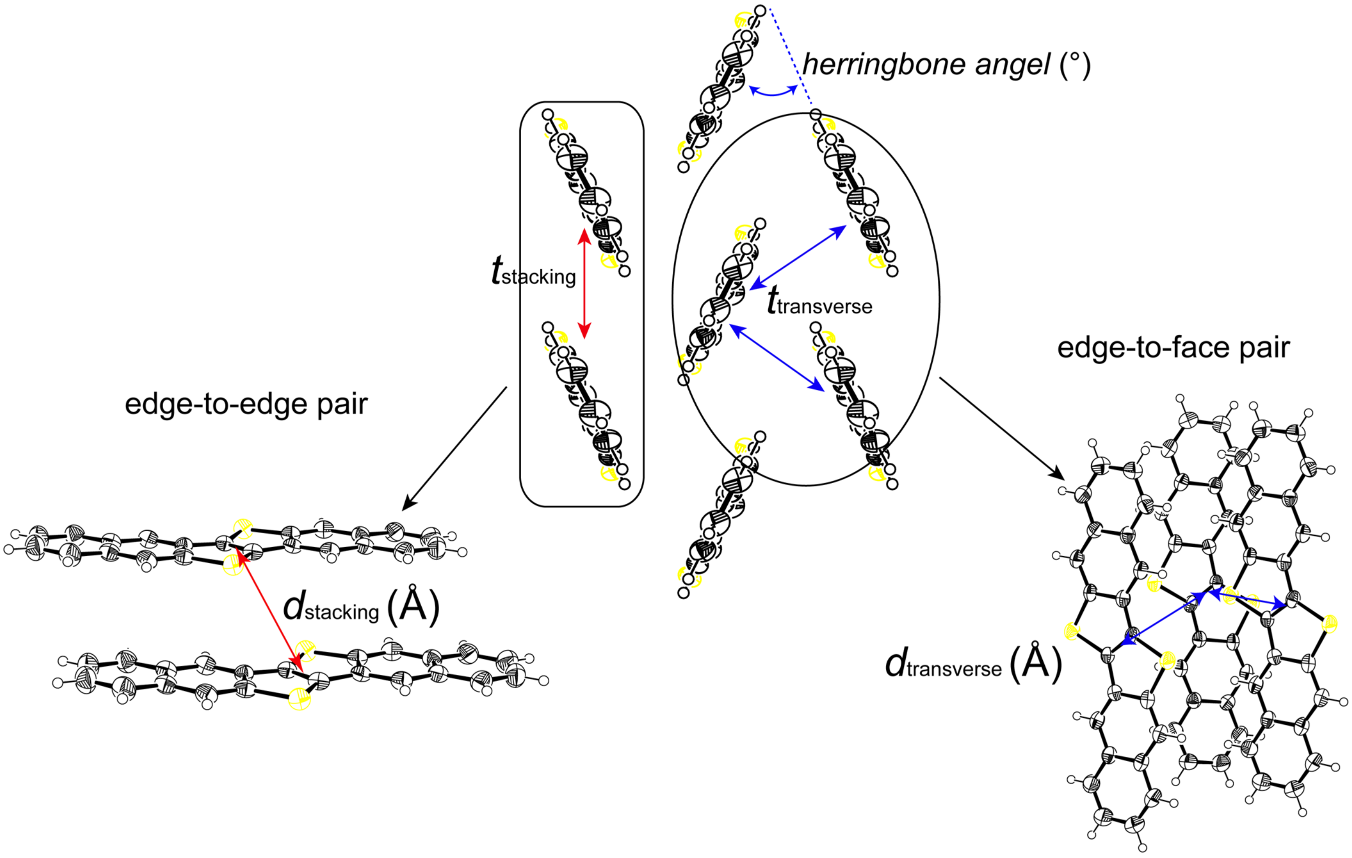

Figure 5. Definitions of intermolecular factors in molecular pairs for analysis of the herringbone packing of BTBT-based molecules.

Table 3. Calculated Transfer Integrals (t, meV) and Distance between Molecular Centroids (d, Å) in the Packing Structure

	edge-to-edge pair		edge-to-face pair		
compd	t_{stacking}/meV[a]	d_{stacking}/Å	$t_{\text{transverse}}$/meV[a]	$d_{\text{transverse}}$/Å	herringbone angle/deg
BTBT	60	5.89	23	5.00	58.5
DPh-BTBT	34	6.33	65	4.89	42.4
C_{12}-BTBT	62	5.99	46	4.86	55.2
DNTT[b]	71	6.19	91	4.93	52.6
			14	5.10	
2,9-C_{10}-DNTT	83	5.99	51	4.85	51.1
2,9-DPh-DNTT	52	6.18	45	4.90	46.5
3,10-DPh-DNTT	22	6.99	80	5.01	34.5
DATT[b]	70	6.26	88	4.92	51.4
			35	5.15	

[a] Transfer integrals (t's) were calculated using the Amsterdam Density Functional (ADF) program package. [b] Owing to lower symmetry of the unit cells, two independent edge-to-face pairs exist and thus two different $t_{\text{transverse}}$'s are calculated.

From the above inspection of the packing structures, it can be concluded that molecular factors, such as molecular size and substituent, can alter the mutual positions of molecules in the solid state and hence the extent of intermolecular orbital overlaps. In fact, the large molecular size and alkylation are advantageous for enhancing the orbital overlap. On the other hand, the introduction of phenyl groups set the molecules apart in the edge-to-edge pairs and weakens the intermolecular orbital overlap in this direction, although the extent of such effects is dependent on the substitution position. As a result, the molecular factors cause subtle changes in the resulting intermolecular orbital overlaps, although the present BTBT-based materials can afford mostly a 2D isotropic electronic structure with relatively large intermolecular orbital overlaps in the solid state. These structural characterizations can rationalize the high mobilities of OFETs fabricated with polycrystalline thin films as the active layer.

5. SUMMARY AND OUTLOOK

Our initial working hypothesis that thiophene-based molecules possessing HOMO largely contributed by sulfur atoms should be potential organic semiconductors prompted us to examine BTBT-based materials. Although the hypothesis could be rather naive, the BTBT-based materials have turned out to be superior organic semiconductors for OFETs. The features of the present material class, that is, low-lying HOMO energy level, good chemical stability, and high carrier mobility of OFET devices with various device configurations, originate from the thienothiophene moiety incorporated in the middle of the π-conjugated core. As a result, the present BTBT-based materials can be regarded as one of the ideal classes of p-channel organic semiconductors from both experimental and theoretical viewpoints. We hope that these materials will contribute to the development of practical applications for OFETs, and the BTBT and related thienoacene structures will be a platform for the further development of superior organic semiconductors. In addition, we also hope that the concept of materials design discussed here will provide hints to develop further superior materials. In fact, new thienoacene-based organic semiconductors with fused benzene and thiophene rings recently developed show very high mobility close to or exceeding 10 $cm^2\ s^{-1}\ V^{-1}$,[37] which will expand organic semiconductors' horizons.

■ ASSOCIATED CONTENT

Ⓢ Supporting Information

Computational details. This material is available free of charge via the Internet at http://pubs.acs.org.

■ AUTHOR INFORMATION

Corresponding Author

*E-mail: takimiya@riken.jp.

Notes

The authors declare no competing financial interest.

Biographies

Kazuo Takimiya is the Group Director at RIKEN Center for Emergent Matter Science (CEMS). He obtained his Ph.D. from Hiroshima University in 1994 under the supervision of Professor F. Ogura. Thereafter, he joined Professor T. Otsubo's group at Hiroshima University where he studied organic conductors/superconductors. He was promoted to associate professor in 2003 and to full professor in 2007 at Hiroshima University. In 2013, his group moved to RIKEN. His current research interests include the syntheses, characterization, and application of organic semiconductors.

Itaru Osaka received his Ph.D. from the University of Tsukuba in 2002. After a 4-year research stint at Fujifilm, he joined Professor R. D. McCullough's group at Carnegie Mellon University as a postdoctoral fellow. He then joined Professor Takimiya's group at Hiroshima University as an assistant professor in 2009, and moved to RIKEN CEMS as a senior research scientist in 2013. His research interests include the design and synthesis of conjugated polymers for organic electronics.

Masahiro Nakano received his Ph.D. from Hiroshima University in 2013. He is currently a postdoctoral fellow of Japan Society for the Promotion of Science (JSPS) and belongs to the Emergent Molecular Function Research Group at RIKEN CEMS. His current research focuses on the synthesis and application of organic semiconductors.

Takamichi Mori received his bachelor's degree from Hiroshima University in 2012 under the supervision of Professor Takimiya. He is continuing his studies on organic semiconductors in the Emergent Molecular Function Research Group at RIKEN CEMS as a visiting student.

■ ACKNOWLEDGMENTS

This work was financially supported by a Grant-in-Aid for Scientific Research (No. 23245041) from MEXT, Japan. M.N. is indebted to JSPS for his postdoctoral fellowship.

■ REFERENCES

(1) (a) The Special Issue on Organic Electronics. *Chem. Mater.* **2004**, *16*, 4381−4382. (b) Bredas, J.-L.; Marder, S. R.; Reichmanis, E. Preface to the Chemistry of Materials Special Issue on π-Functional Materials. *Chem. Mater.* **2011**, *23*, 309−309.

(2) Bao, Z., Locklin, J., Eds. *Organic Field-Effect Transistors*; CRC Press: Boca Raton, FL, 2007.

(3) Horowitz, G.; Peng, X.-Z.; Fichou, D.; Garnier, F. Role of the semiconductor/insulator interface in the characteristics of π-conjugated-oligomer-based thin-film transistors. *Synth. Met.* **1992**, *51*, 419−424.

(4) Kelley, T. W.; Boardman, L. D.; Dunbar, T. D.; Muyres, D. V.; Pellerite, M. J.; Smith, T. P. High-Performance OTFTs Using Surface-Modified Alumina Dielectrics. *J. Phys. Chem. B* **2003**, *107*, 5877−5881.

(5) *Organic Electronics, Manufacturing and Applications*; Klauk, H., Ed.; Wiley-VCH: Weinheim, 2006.

(6) (a) Anthony, J. E. Functionalized Acenes and Heteroacenes for Organic Electronics. *Chem. Rev.* **2006**, *106*, 5028−5048. (b) Anthony, J. E. The Larger Acenes: Versatile Organic Semiconductors. *Angew. Chem., Int. Ed.* **2008**, *47*, 452−483.

(7) (a) Murphy, A. R.; Fréchet, J. M. J. Organic Semiconducting Oligomers for Use in Thin Film Transistors. *Chem. Rev.* **2007**, *107*, 1066−1096. (b) Mei, J.; Diao, Y.; Appleton, A. L.; Fang, L.; Bao, Z. Integrated Materials Design of Organic Semiconductors for Field-Effect Transistors. *J. Am. Chem. Soc.* **2013**, *135*, 6724−6746.

(8) (a) Meng, H.; Bao, Z.; Lovinger, A. J.; Wang, B.-C.; Mujsce, A. M. High Field-Effect Mobility Oligofluorene Derivatives with High Environmental Stability. *J. Am. Chem. Soc.* **2001**, *123*, 9214−9215.

(9) Brédas, J.-L.; Beljonne, D.; Coropceanu, V.; Cornil, J. Charge-Transfer and Energy-Transfer Processes in π-Conjugated Oligomers and Polymers: A Molecular Picture. *Chem. Rev.* **2004**, *104*, 4971−5004.

(10) (a) Katz, H. E.; Torsi, L.; Dodabalapur, A. Synthesis, Material Properties, and Transistor Performance of Highly Pure Thiophene Oligomers. *Chem. Mater.* **1995**, *7*, 2235−2237. (b) Horowitz, G.; Garnier, F.; Yassar, A.; Hajlaoui, R.; Kouki, F. Field-effect transistor made with a sexithiophene single crystal. *Adv. Mater.* **1996**, *8*, 52−54.

(11) (a) Laquindanum, J. G.; Katz, H. E.; Lovinger, A. J.; Dodabalapur, A. Benzodithiophene Rings as Semiconductor Building Blocks. *Adv. Mater.* **1997**, *9*, 36−39. (b) Li, X.-C.; Sirringhaus, H.; Garnier, F.; Holmes, A. B.; Moratti, S. C.; Feeder, N.; Clegg, W.; Teat, S. J.; Friend, R. H. A Highly π-Stacked Organic Semiconductor for Thin Film Transistors Based on Fused Thiophenes. *J. Am. Chem. Soc.* **1998**, *120*, 2206−2207.

(12) Horton, A. W. The Mechanism of The Reactions of Hydrocarbons with Sulfur 1. *J. Org. Chem.* **1949**, *14*, 761−770.

(13) Košata, B.; Kozmík, V.; Svoboda, J. Reactivity of [1]-Benzothieno[3,2-*b*][1]benzothiophene - Electrophilic and Metallation Reactions. *Collect. Czech. Chem. Commun.* **2002**, *67*, 645−664.

(14) Saito, M.; Osaka, I.; Miyazaki, E.; Takimiya, K.; Kuwabara, H.; Ikeda, M. One-step synthesis of [1]benzothieno[3,2-*b*][1]-benzothiophene from *o*-chlorobenzaldehyde. *Tetrahedron Lett.* **2011**, *52*, 285−288.

(15) Sashida, H.; Yasuike, S. A simple one-pot synthesis of [1]benzotelluro[3,2-*b*][1]benzotellurophenes and its selenium and sulfur analogues from 2,2′-dibromodiphenylacetylene. *J. Heterocycl. Chem.* **1998**, *35*, 725−726.

(16) Zherdeva, S. Y.; Barudi, A.; Zheltov, A. Y.; Stepanov, B. I. Synthesis and transformations of benzo[3,2-*b*]benzothiophenes. *Zh. Org. Khim.* **1980**, *16*, 430−438.

(17) Kaszynski, P.; Dougherty, D. A. Synthesis and properties of diethyl 5,10-dihetera-5,10-dihydroindeno[2,1-*a*]indene-2,7-dicarboxylates. *J. Org. Chem.* **1993**, *58*, 5209−5220.

(18) Ruzié, C.; Karpinska, J.; Kennedy, A. R.; Geerts, Y. H. Synthesis of 1,6-, 2,7-, 3,8-, and 4,9-Isomers of Didodecyl[1]benzothieno[3,2-*b*][1]benzothiophenes. *J. Org. Chem.* **2013**, *78*, 7741−7748.

(19) Takimiya, K.; Ebata, H.; Sakamoto, K.; Izawa, T.; Otsubo, T.; Kunugi, Y. 2,7-Diphenyl[1]benzothieno[3,2-*b*]benzothiophene, A New Organic Semiconductor for Air-Stable Organic Field-Effect Transistors with Mobilities up to 2.0 $cm^2\ V^{-1}\ s^{-1}$. *J. Am. Chem. Soc.* **2006**, *128*, 12604−12605.

(20) (a) Ebata, H.; Izawa, T.; Miyazaki, E.; Takimiya, K.; Ikeda, M.; Kuwabara, H.; Yui, T. Highly Soluble [1]Benzothieno[3,2-*b*]-benzothiophene (BTBT) Derivatives for High-Performance, Solution-Processed Organic Field-Effect Transistors. *J. Am. Chem. Soc.* **2007**, *129*, 15732−15733. (b) Izawa, T.; Miyazaki, E.; Takimiya, K. Molecular Ordering of High-Performance Soluble Molecular Semiconductors and Re-evaluation of Their Field-Effect Transistor Characteristics. *Adv. Mater.* **2008**, *20*, 3388−3392.

(21) (a) Iino, H.; Kobori, T.; Hanna, J.-i. Improved thermal stability in organic FET fabricated with a soluble BTBT derivative. *J. Non-Cryst. Solids* **2012**, *358*, 2516−2519. (b) Amin, A. Y.; Khassanov, A.; Reuter, K.; Meyer-Friedrichsen, T.; Halik, M. Low-Voltage Organic Field Effect Transistors with a 2-Tridecyl[1]benzothieno[3,2-*b*][1]-benzothiophene Semiconductor Layer. *J. Am. Chem. Soc.* **2012**, *134*, 16548−16550.

(22) Yamamoto, T.; Takimiya, K. Facile Synthesis of Highly π-Extended Heteroarenes, Dinaphtho[2,3-*b*:2′,3′-*f*]chalcogenopheno-[3,2-*b*]chalcogenophenes, and Their Application to Field-Effect Transistors. *J. Am. Chem. Soc.* **2007**, *129*, 2224−2225.

(23) (a) Kuribara, K.; Wang, H.; Uchiyama, N.; Fukuda, K.; Yokota, T.; Zschieschang, U.; Jaye, C.; Fischer, D.; Klauk, H.; Yamamoto, T.; Takimiya, K.; Ikeda, M.; Kuwabara, H.; Sekitani, T.; Loo, Y.-L.; Someya, T. Organic transistors with high thermal stability for medical applications. *Nat. Commun.* **2012**, *3*, 723. (b) Kaltenbrunner, M.; Sekitani, T.; Reeder, J.; Yokota, T.; Kuribara, K.; Tokuhara, T.; Drack, M.; Schwodiauer, R.; Graz, I.; Bauer-Gogonea, S.; Bauer, S.; Someya, T. An ultra-lightweight design for imperceptible plastic electronics. *Nature* **2013**, *499*, 458−463.

(24) Kang, M. J.; Doi, I.; Mori, H.; Miyazaki, E.; Takimiya, K.; Ikeda, M.; Kuwabara, H. Alkylated Dinaphtho[2,3-*b*:2′,3′-*f*]Thieno[3,2-*b*]Thiophenes (C_n-DNTTs): Organic Semiconductors for High-Performance Thin-Film Transistors. *Adv. Mater.* **2011**, *23*, 1222−1225.

(25) Niimi, K.; Kang, M. J.; Miyazaki, E.; Osaka, I.; Takimiya, K. General Synthesis of Dinaphtho[2,3-*b*:2′,3′-*f*]thieno[3,2-*b*]thiophene (DNTT) Derivatives. *Org. Lett.* **2011**, *13*, 3430−3433.

(26) Niimi, K.; Shinamura, S.; Osaka, I.; Miyazaki, E.; Takimiya, K. Dianthra[2,3-*b*:2′,3′-*f*]thieno[3,2-*b*]thiophene (DATT): Synthesis, Characterization, and FET Characteristics of New π-Extended Heteroarene with Eight Fused Aromatic Rings. *J. Am. Chem. Soc.* **2011**, *133*, 8732−8739.

(27) (a) Yamamoto, T.; Nishimura, T.; Mori, T.; Miyazaki, E.; Osaka, I.; Takimiya, K. Largely π-Extended Thienoacenes with Internal Thieno[3,2-*b*]thiophene Substructures: Synthesis, Characterization, and Organic Field-Effect Transistor Applications. *Org. Lett.* **2012**, *14*, 4914−4917. (b) Mori, T.; Nishimura, T.; Yamamoto, T.; Doi, I.; Miyazaki, E.; Osaka, I.; Takimiya, K. Consecutive Thiophene-Annulation Approach to π-Extended Thienoacene-Based Organic Semiconductors with [1]Benzothieno[3,2-*b*][1]benzothiophene (BTBT) Substructure. *J. Am. Chem. Soc.* **2013**, *135*, 13900−13913.

(28) (a) Inokuchi, H.; Saito, G.; Wu, P.; Seki, K.; Tang, T. B.; Mori, T.; Imaeda, K.; Enoki, T.; Higuchi, Y.; Inaka, K.; Yasuoka, N. A Novel Type of Organic Semiconductors. Molecular Fastener. *Chem. Lett.* **1986**, *15*, 1263−1266. (b) Nan, G.; Li, Z. Crystal structure versus charge transport in organic single crystals of [1]benzothieno[3,2-*b*][1]benzothiophene derivatives from a multiscale theoretical study. *J. Mater. Chem. C* **2014**, *2*, 1447−1456.

(29) Takimiya, K.; Yamamoto, T.; Ebata, H.; Izawa, T. Design strategy for air-stable organic semiconductors applicable to high-performance field-effect transistors. *Sci. Technol. Adv. Mater.* **2007**, *8*, 273−276.

(30) (a) Endo, T.; Nagase, T.; Kobayashi, T.; Takimiya, K.; Ikeda, M.; Naito, H. Solution-Processed Dioctylbenzothienobenzothiophene-Based Top-Gate Organic Transistors with High Mobility, Low Threshold Voltage, and High Electrical Stability. *Appl. Phys. Express* **2010**, *3*, 121601. (b) Kano, M.; Minari, T.; Tsukagoshi, K. All-Solution-Processed Selective Assembly of Flexible Organic Field-Effect Transistor Arrays. *Appl. Phys. Express* **2010**, *3*, 051601. (c) Liu, C.; Minari, T.; Lu, X.; Kumatani, A.; Takimiya, K.; Tsukagoshi, K. Solution-Processable Organic Single Crystals with Bandlike Transport in Field-Effect Transistors. *Adv. Mater.* **2011**, *23*, 523−526. (d) Uemura, T.; Hirose, Y.; Uno, M.; Takimiya, K.; Takeya, J. Very High Mobility in Solution-Processed Organic Thin-Film Transistors of Highly Ordered [1]Benzothieno[3,2-*b*]benzothiophene Derivatives. *Appl. Phys. Express* **2009**, *2*, 111501. (e) Minemawari, H.; Yamada, T.; Matsui, H.; Tsutsumi, J. y.; Haas, S.; Chiba, R.; Kumai, R.; Hasegawa, T. Inkjet printing of single-crystal films. *Nature* **2011**, *475*, 364−367.

(31) Haas, S.; Takahashi, Y.; Takimiya, K.; Hasegawa, T. High-performance dinaphtho-thieno-thiophene single crystal field-effect transistors. *Appl. Phys. Lett.* **2009**, *95*, 022111.

(32) (a) Uno, M.; Hirose, Y.; Uemura, T.; Takimiya, K.; Nakazawa, Y.; Takeya, J. High-power and high-speed organic three-dimensional transistors with submicrometer channels. *Appl. Phys. Lett.* **2010**, *97*, 013301. (b) McCarthy, M. A.; Liu, B.; Donoghue, E. P.; Kravchenko, I.; Kim, D. Y.; So, F.; Rinzler, A. G. Low-Voltage, Low-Power, Organic Light-Emitting Transistors for Active Matrix Displays. *Science* **2011**, *332*, 570−573. (c) Zschieschang, U.; Ante, F.; Yamamoto, T.; Takimiya, K.; Kuwabara, H.; Ikeda, M.; Sekitani, T.; Someya, T.; Kern, K.; Klauk, H. Flexible Low-Voltage Organic Transistors and Circuits Based on a High-Mobility Organic Semiconductor with Good Air Stability. *Adv. Mater.* **2010**, *22*, 982−985.

(33) Ante, F.; Kälblein, D.; Zschieschang, U.; Canzler, T. W.; Werner, A.; Takimiya, K.; Ikeda, M.; Sekitani, T.; Someya, T.; Klauk, H. Contact Doping and Ultrathin Gate Dielectrics for Nanoscale Organic Thin-Film Transistors. *Small* **2011**, 1186−1191.

(34) Kang, M. J.; Miyazaki, E.; Osaka, I.; Takimiya, K.; Nakao, A. Diphenyl Derivatives of Dinaphtho[2,3-*b*:2′,3′-*f*]thieno[3,2-*b*]-thiophene: Organic Semiconductors for Thermally Stable Thin-Film Transistors. *ACS Appl. Mater. Interfaces* **2013**, *5*, 2331−2336.

(35) Yokota, T.; Kuribara, K.; Tokuhara, T.; Zschieschang, U.; Klauk, H.; Takimiya, K.; Sadamitsu, Y.; Hamada, M.; Sekitani, T.; Someya, T. Flexible Low-Voltage Organic Transistors with High Thermal Stability at 250 °C. *Adv. Mater.* **2013**, *25*, 3639−3644.

(36) Valiyev, F.; Hu, W.-S.; Chen, H.-Y.; Kuo, M.-Y.; Chao, I.; Tao, Y.-T. Synthesis and Characterization of Anthra[2,3-*b*]thiophene and Tetraceno[2,3-*b*]thiophenes for Organic Field-Effect Transistor Applications. *Chem. Mater.* **2007**, *19*, 3018−3026.

(37) (a) Kurihara, N.; Yao, A.; Sunagawa, M.; Ikeda, Y.; Terai, K.; Kondo, H.; Saito, M.; Ikeda, H.; Nakamura, H. High-Mobility Organic Thin-Film Transistors Over 10 cm^2 s^{-1} V^{-1} Fabricated Using Bis(benzothieno)naphthalene Polycrystalline Films. *Jpn. J. Appl. Phys.* **2013**, *52*, 05DC11. (b) Okamoto, T.; Mitsui, C.; Yamagishi, M.; Nakahara, K.; Soeda, J.; Hirose, Y.; Miwa, K.; Sato, H.; Yamano, A.; Matsushita, T.; Uemura, T.; Takeya, J. V-Shaped Organic Semiconductors With Solution Processability, High Mobility, and High Thermal Durability. *Adv. Mater.* **2013**, *25*, 6392−6397.